Green Chemistry



PAPER



Cite this: Green Chem., 2023, 25. 10082

Received 28th August 2023, Accepted 13th November 2023 DOI: 10.1039/d3qc03249c

rsc.li/greenchem

Synthesis and properties of linseed oil-based waterborne non-isocyanate polyurethane coating†

Zichen Ling and Qixin Zhou **

Significant strides in the development of non-isocyanate polyurethane (NIPU) have been made in the coatings industry. Aligned with green chemistry principles, this study explores the use of bio-based, low volatile organic compounds and fast-curing waterborne NIPU for coating applications. The linseed oilbased cyclic carbonate was synthesized via a thiol-ene click reaction and was followed by an esterification reaction directly from linseed oil. In this structure, the cyclic carbonates are introduced as pendant functional groups to accelerate the curing. Next, a series of linseed oil-based waterborne NIPUs were synthesized and developed from the linseed oil-based cyclic carbonate, a bio-based fatty acid diamine, and an internal dispersion agent. Different formulations of the linseed oil-based NIPU coatings were designed by varying the internal dispersion agent content and urethane content, and a solvent-borne NIPU was included in the study for comparison purposes. The NIPU coatings with different formulations achieved a broad range of thermal stabilities, viscoelastic properties, and mechanical properties. The general coating properties-including hardness, solvent resistance, impact resistance, and adhesion-were evaluated to demonstrate the practical application of the waterborne NIPU in coatings. The linseed oil-based waterborne NIPU coatings exhibited performance comparable to both a solvent-borne NIPU coating and a commercial waterborne isocyanate-based polyurethane coating

Introduction

Polyurethane (PU) is a versatile material used in many applications such as sensors, medical dressings, food packaging, foams, and coatings; 1-5 the global market for this material was valued at over \$70 billion in 2021 and is expected to increase at a rate of 4.5% per year.6 In general, traditional PU shows excellent properties because of the presence of hydrogen bonding and alternately arranged soft and hard segments,⁷ and it has mainly been obtained from the polyaddition between polyisocyanates and polyols. Unfortunately, isocyanates such as toluene diisocyanate and methylene diphenyl diisocyanate are hazardous to both human health and the environment, and the phosgene used as the precursor of isocyanate is highly toxic. Due to these concerns, the use of nonisocyanate polyurethane (NIPU) has attracted great interest from academia and industry.

The synthesis of NIPU was first reported by Dyer and Scott in 1957, who found that cyclic carbonate reacted with amines

Department of Chemical, Biomolecular, and Corrosion Engineering, The University of Akron, Akron, Ohio, 44325, USA. E-mail: qzhou@uakron.edu

†Electronic supplementary information (ESI) available: 13C NMR spectra for LOAC and LOCC, FTIR spectra of NIPU prepolymer, the particle size distributions of waterborne NIPU dispersions, and viscosity of NIPU dispersions and commercial WPU. See DOI: https://doi.org/10.1039/d3gc03249c

to form urethane groups.8 At present, this cyclic carbonate/ amine reaction is still the most promising method for producing NIPU because of the optimal atom economy of 100%, the numerous choices for raw materials, and properties that are analogous to traditional PU.9,10 The side hydroxyl groups that form from the cyclic carbonate/amine reaction increase the hydrogen bonding density to strengthen the mechanical properties and chemical resistance of NIPU.11-13 However, the cyclic carbonate possesses low reactivity with the amine.14 This issue was addressed in our prior work, where we incorporated an epoxy chain extender, capitalizing on the elevated reaction rate between amine and epoxy.15 Yet, in contrast, a majority of industrial epoxies originate from epichlorohydrin, which is considered to be a carcinogen and has been found to exhibit estrogenic effects on humans. 16 Hence, it is imperative to explore greener and more sustainable alternatives to increase the reactivity of cyclic carbonate for NIPU production.

Recently, vegetable oil has been one of the most promising materials to use for NIPU production, as its benefits include biodegradability, low cost, low toxicity, and low greenhouse emissions during production. 17-19 In addition, vegetable oil has a flexible long chain structure that allows it to act as a soft segment of PU. Moreover, the unsaturation and triglyceride groups of vegetable oil make it possible to be modified for PU synthesis and structure design.20 For example, the double bonds in vegetable oil can be epoxied followed by a ring

opening to obtain bio-based polyol for the preparation of conventional PU.^{21–23} In an alternative process, vegetable oil could first be epoxied and then carbonated by CO₂ under catalysis to produce vegetable oil-based cyclic carbonate for the synthesis of NIPU.^{24,25} Zhang *et al.* prepared a plant oil-based cyclic carbonate by carbonating the epoxidized plant oil, subsequently yielding waterborne NIPUs.²⁶ Nonetheless, akin to numerous NIPUs synthesized *via* the cyclic carbonate ring-opening reaction, the resulting NIPU products typically necessitate a process that involves curing at relatively high temperatures and requires several days due to the formation of internal cyclic carbonate as well as steric hindrance arising from the long chain structure.^{27–29}

The thiol-ene reaction is another avenue for modifying vegetable oil and offers a high reaction rate and yield.³⁰ Jia et al. modified tung oil to tung oil-based polyol through a thiol-ene reaction, then epoxied the polyol with epichlorohydrin to obtain a tung oil-derived epoxy plasticizer.³¹ In another study, Mokhtari and co-workers synthesized jojoba and castor oil-based acids with a pendant carboxyl group through a thiolene reaction. These acids were then subjected to esterification to produce vegetable oil-based cyclic carbonates.³² The synthesized cyclic carbonate displayed enhanced reactivity when reacted with an amine to synthesize NIPU, in comparison to cyclic carbonate obtained through the epoxidation/carbonation method. The enhanced reactivity can be attributed to the presence of pendant cyclic carbonate. However, because the NIPU synthesized from vegetable oil-based cyclic carbonates employed organic solvents, it was classified as a solvent-based NIPU.

Waterborne polyurethane has garnered considerable interest because it can achieve low volatile organic compounds. Waterborne polyurethanes are classified into three groups—cationic, anionic, and nonionic—based on the charge of the neutralized emulsifier. Although anionic and nonionic waterborne polyurethanes occupy most of the market, cationic waterborne polyurethanes demonstrate great application potential due to their excellent adhesion and antibacterial properties, among other benefits. Therefore, the innovative aspect of this study lies in the synthesis of a cationic waterborne NIPU using a vegetable oil-based cyclic carbonate with higher reactivity, ultimately leading to reduced curing time.

In this paper, we describe the formulation of a series of waterborne NIPUs from a linseed oil-based cyclic carbonate featuring pendant cyclic carbonates in conjunction with biobased fatty acid amine (FDA) and 3,3'-diamino-N methyldipropylamine (DMDPA). Linseed oil, which is derived from flax seeds, is chosen as the precursor for chemical modification due to its eco-friendliness, sustainability, and high content of unsaturated double bonds. Herein, linseed oil is first reacted with thioglycolic acid to produce linseed oil acid (LOAC) through a thiol–ene reaction and is subsequently reacted with glycerol carbonate to produce linseed oil cyclic carbonate (LOCC), which harbors pendant cyclic carbonate groups. Different NIPU formulations were designed to tune the properties of the waterborne NIPU. The chemical structure of the

LOCC was validated by Fourier transform infrared spectroscopy (FTIR) and 1 H and 13 C nuclear magnetic resonance spectroscopy (NMR). The glass transition temperatures ($T_{\rm g}$) of the NIPU coating films were characterized by differential scanning calorimetry (DSC), and their thermal stability was studied by thermogravimetric analysis (TGA). Viscoelastic and mechanical properties were determined using dynamic mechanical thermal analysis (DMTA) and tensile tests. General coating properties such as hardness, solvent resistance, impact resistance, and adhesion were also evaluated.

Experimental

Materials

Linseed oil, thioglycolic acid (98%, 92.12 g mol⁻¹), 1,1'-carbonyldiimidazole (CDI, \geq 97.0%, 162.15 g mol⁻¹), 2,2'-azobis(2methylpropionitrile) (AIBN) (98%, 164.21 g mol⁻¹), 3,3'diamino-N-methyldipropylamine (96%, 145.25 g mol⁻⁻¹), sodium hydroxide (NaOH, ≥97.0%, 40.00 g mol⁻¹), methyl ethyl ketone (MEK) (\geq 99.0%, 72.11 g mol⁻¹), and dichloromethane $(CH_2Cl_2, \geq 99.9\%, 84.93 \text{ g mol}^{-1})$ were purchased from Sigma-Aldrich. Ethyl acetate (≥99.5%, 88.106 g mol⁻¹) and magnesium sulfate (MgSO₄) were purchased from Fisher Scientific. Glycerol-1,2-carbonate ($\geq 90.0\%$, 118.09 g mol⁻¹), sodium chloride (NaCl, ≥99.0%, 58.44 g mol⁻¹), and hydrochloric acid (HCl, 37%) were purchased from VWR International. PriamineTM 1075-LQ-(GD) dimer fatty acid diamine was provided by Croda International. The commercial waterborne PU (Varathane 200241H water-based ultimate polyurethane) was purchased from Amazon. All materials were used as received without further purification.

Synthesis procedure

Synthesis of linseed oil cyclic carbonate

The synthesis of linseed oil cyclic carbonate (LOCC) shown in Scheme 1 is similar to that in a previous report. First, 70.0 g linseed oil and 7.78 g AIBN were mixed by magnetic stirring in an $\rm N_2$ atmosphere. Next, 130.0 g of thioglycolic acid was dropped into the mixture to achieve a thiol/ene/AIBN molar ratio of around 3:1:0.1. The mixture was heated to 80 °C for 6 h to obtain linseed oil acid (LOAC). After the reaction, the product was dissolved in ethyl acetate and washed three times with saturated NaCl solution. The organic layer was collected and then dried using magnesium sulfate, filtration, and solvent removal with a rotary evaporator.

The linseed oil cyclic carbonate (LOCC) was synthesized by the esterification between LOAC and glycerol carbonate. First, $35.0~\rm g$ of LOAC was dissolved in $\rm CH_2Cl_2$ in a three-neck round-bottom flask under $\rm N_2$ purge. The flask was placed in an ice bath, and $38.8~\rm g$ of 1,1'-carbonyldiimidazole (CDI) was added to the mixture. Next, $28.2~\rm g$ of glycerol-1,2-carbonate was dropped into the flask for around $0.5~\rm h$. After the flask was removed from the ice bath, the mixture was permitted to react

Scheme 1 The synthesis procedure of LOCC.

at room temperature for 20 h. The product was then collected by liquid–liquid extraction with ethyl acetate and was washed three times with 0.5 N HCl solution and 0.5 N NaOH solution. Finally, the organic layer was collected and dried using MgSO₄, filtration, and solvent removal with a rotary evaporator.

linseed oil cyclic carbonate (LOCC)

Synthesis of solvent-borne NIPU

First, LOCC was dissolved in MEK followed by the addition of FDA. Next, the mixture was heated to 75 °C for 2 h. The product was named NIPU-1, and the formulation details are listed in Table 1. NIPU-1 was designed as a control to facilitate the comparison of its properties to those of waterborne NIPUs.

Synthesis of waterborne NIPU

Three different waterborne NIPUs were designed by changing the content of the internal emulsifier (DMDPA), and their com-

Table 1 The composition details of NIPU (wt%)

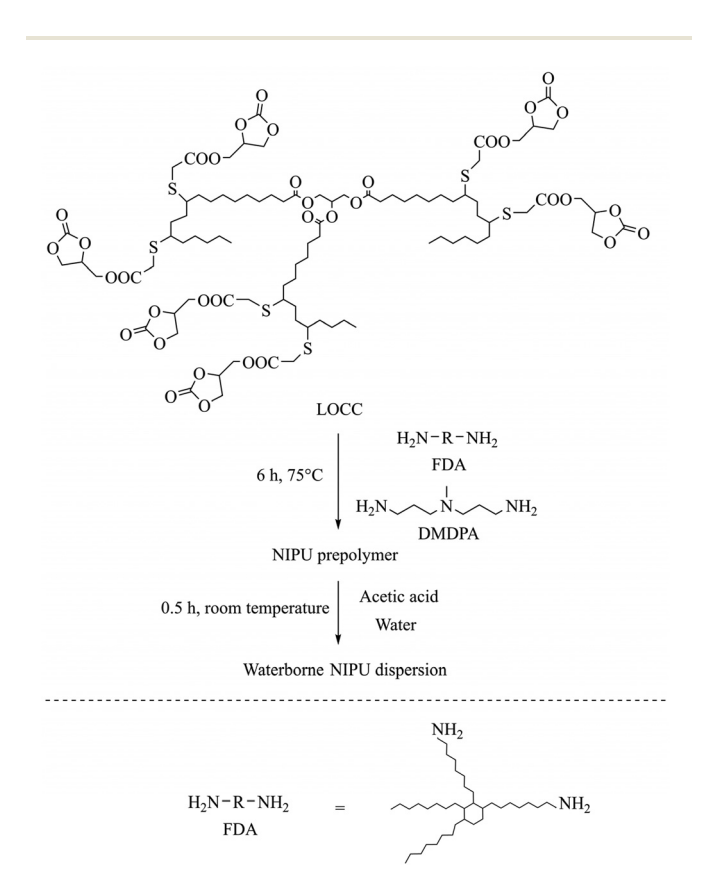
	LOCC	FDA	DMDPA
NIPU-1	55	45	_
NIPU-2	63	32	5
NIPU-3	70	20	10
NIPU-4	78	7	15

The molar ratio of cyclic carbonate to amine group is 1:1.

positions are provided in Table 1. The molar ratio of the amine group to cyclic carbonate was kept at 1:1 for all NIPUs based on the theoretical functionality of LOCC. The synthesis procedure of the waterborne NIPUs is shown in Scheme 2. In this procedure, LOCC, FDA, and DMDPA were first mixed in MEK under an N_2 atmosphere, and the mixture was reacted at 75 °C for 6 h. Next, acetic acid with the same amount of DMDPA was added to the mixture to neutralize the product. After 0.5 h, the product was dispersed in water by a mechanical stirrer with a speed of 500 rpm for a period of 1 h, followed by solvent removal, which was accomplished using a rotary evaporator. The solid content of the dispersion was around 15–18 wt%.

Preparation of NIPU coatings

After the synthesis of the NIPUs, the dispersions were applied on QD-36 steel substrates (Q-Lab Corporation) by a drawdown



Scheme 2 The synthesis procedure of waterborne NIPU.

bar to a wet film thickness of 150 μm . The QD-36 substrates were rinsed with acetone and were air-dried prior to use. The resulting samples were maintained at room temperature overnight before being cured at 120 °C for 6 h to form tack-free films. Once the coatings had cured, the dry film thickness was measured using an Elcometer digital coating thickness gauge.

Characterization methods

FTIR spectra for all samples were obtained by a Nicolet iS10 FTIR spectrometer at room temperature with an attenuated total reflection mode of 64 scans and a resolution of 4 cm $^{-1}$. The $^1\mathrm{H}$ and $^{13}\mathrm{C}$ NMR spectra were obtained by a Varian INOVA 300 spectrometer at room temperature using CDCl $_3$ as the solvent.

The iodine values (*i.e.*, the quantity of iodine, in grams, sufficient to react with 100 grams of a sample) of linseed oil and LOAC were determined according to the Wijs method using ISO 3961:2018. The acid value of LOAC was determined by acid-base titration, in which 0.3 g of LOAC was dissolved in 50 mL isopropyl alcohol, and 1 mL phenolphthalein (1% w/v) was dropped as an indicator. The resulting solution was titrated with 0.1 N potassium hydroxide (KOH). The acid value was calculated as:

$$A = \frac{56.1 \times V \times C}{W} \tag{1}$$

where A is the acid value (KOH g g⁻¹), V is the volume of titrant used, C is the molarity of the KOH solution, and W is the weight of the sample.

The carbonate equivalent weight (CEW) is the amount of product containing one equivalent of cyclic carbonate. The CEW was determined by the ¹H NMR spectra using benzophenone as the internal reference. ³⁶ Known amounts of benzophenone and LOCC were dissolved in 0.4 mL CDCl₃ in the NMR tube, and the CEW was determined using the equation below:

$$\begin{aligned} \text{CEW} &= \frac{\int \text{benzophenone}}{\int \text{cyclic carbonate}} \times \frac{H_{\text{cyclic carbonate}}}{H_{\text{benzophenone}}} \times \frac{m_{\text{cyclic carbonate}}}{m_{\text{benzophenone}}} \\ &\times M_{\text{benzophenone}} \end{aligned}$$

Where \int benzophenone is the integration value of the proton signals of benzophenone at 7.4–7.7 ppm, \int cyclic carbonate is the integration value of cyclic carbonate signals at 4.9 ppm, $H_{\rm cyclic\ carbonate}$ is the number of protons in α of the cyclic carbonate group, $H_{\rm benzophenone}$ is the number of benzophenone protons, $m_{\rm cyclic\ carbonate}$ is the weight of LOCC, $m_{\rm benzophenone}$ is the weight of benzophenone, and $m_{\rm benzophenone}$ is the molecular weight of benzophenone.

The stability of the waterborne NIPU dispersion was evaluated by centrifugation (corning LSE compact centrifuge), which was conducted at 3000 rpm for 30 min. Dynamic light scattering using a Malvern ZetaSizer zeta potential analyzer was conducted at room temperature to investigate the particle size distribution of the waterborne NIPUs.

The glass transition temperature ($T_{\rm g}$) of NIPU coating films was determined by differential scanning calorimetry (DSC; TA Instruments Q200) under a nitrogen atmosphere (40 mL min⁻¹) and at a rate of 10 °C min⁻¹. The weight of the samples was around 5 mg. The temperature range was -70 °C to 80 °C.

The thermal stability of NIPU coating films was characterized by thermogravimetric analysis (TGA, TA Instruments Q500). The weight of the samples was around 10 mg. The temperature of each sample was raised to 600 °C at a steady rate of 10 °C min⁻¹ under nitrogen purge (10 mL min⁻¹), and the temperature was maintained at 600 °C for 10 minutes.

The viscoelastic properties of the cured coating films were examined using a TA Instruments Q800 dynamic mechanical thermal analyzer in tension mode with a constant frequency of 1 Hz. The tests were conducted on coating film that was peeled from the substrate and cut into samples that were 15 mm in length and 8 mm in width. The samples were cooled to $-70~\rm ^{\circ}C$ and heated to $80~\rm ^{\circ}C$ at a rate of $3~\rm ^{\circ}C$ min $^{-1}$.

The mechanical properties of NIPU coating films were tested using an Instron 5567 universal testing machine (Instron Corp.) operated at room temperature. Self-standing films were peeled from the substrates and were cut into the desired dimensions for mechanical testing (approximately 30 mm in length and 10 mm in width). The moving speed of the test frame was 5 mm min⁻¹. The average obtained by testing five replicates of each sample is reported.

The viscosity of the polyurethane dispersions was measured using an ARES-G2 rheometer (TA Instruments) with a 25 mm cone-and-plate geometry. The measurement was carried out at 25 °C, using a shear rate ranging from 1 s⁻¹ to 100 s⁻¹. The NIPU coating samples (*i.e.*, the coatings on the steel substrates) were also evaluated for their general coating properties. Other properties that were investigated and the standards that were used included pendulum hardness (ASTM D4366), pencil hardness (ASTM D3363), solvent resistance (ASTM D4752), reverse impact resistance (ISO 6272-2), crosshatch adhesion (ASTM D3359), and pull-off adhesion (ASTM D4541).

Results and discussion

(2)

Characterization of linseed oil acid and linseed oil cyclic carbonate

The synthesis of linseed oil cyclic carbonate (LOCC) involves two steps. The first step is the functionalization of linseed oil with thioglycolic acid to obtain linseed oil acid (LOAC) by thiol–ene click reaction. Here, a thiol/ene molar ratio of 3:1 was selected to obtain the best yield. The iodine values obtained for linseed oil and LOAC were 174 g per 100 g and 1.1 g per 100 g, respectively. The acid value of LOAC was also determined based on the titration, and the obtained acid value of 0.25 KOH g g⁻¹ is in good agreement with the theoretical acid value (0.24 KOH g g⁻¹). The second step in the synthesis is the esterification of LOAC with glycerol-1,2-carbonate catalyzed by CDI to obtain LOCC.

The successful synthesis of LOAC and LOCC was further confirmed by both FTIR and NMR spectra. In the FTIR spectra presented in Fig. 1, the peak at 3010 cm⁻¹ in the linseed oil curve was attributed to double bond stretching, while the peaks at 2923 cm⁻¹ and 2853 cm⁻¹ were assigned to C-H stretching, and the signal at 1742 cm⁻¹ was assigned to the C=O stretching of ester.³⁸ After the conversion of the linseed oil to LOAC, the signal for double bond stretching at 3010 cm⁻¹ disappeared, and a new signal appeared at 1708 cm⁻¹ that was associated with the C=O stretching of acid. In addition, after the esterification of LOAC, a new peak appeared at 1798 cm⁻¹ in the LOCC curve, and this peak was associated with the C=O stretching of cyclic carbonate.³⁹

Nuclear magnetic resonance spectroscopy (both ¹H NMR and ¹³C NMR) also confirmed the chemical structures of the LOAC and LOCC. As shown in Fig. 2(a), the peak in the spectrum for linseed oil at 5.35 ppm belongs to the vinyl protons; this peak disappears in the spectrum for LOAC, as shown in Fig. 2(b), and two new peaks are generated: one at 2.75 ppm that corresponds to the proton in CH-S and another at 3.21 ppm that corresponds to the proton linked to the acid group. 37,40 The spectrum for LOCC, shown in Fig. 2(c), exhibits peaks at 4.96, 4.57, and 4.26-4.46 ppm that are associated with the protons of cyclic carbonate. The equivalent weight of the cyclic carbonate was also characterized by ¹H NMR, and the carbonate equivalent weight of LOCC was 351 g eq⁻¹. Given the theoretical molecular weight of LOCC (1988 g mol⁻¹), the functionality of LOCC was determined to be 5.7. Fig. S1(a)† shows the ¹³C NMR spectra of LOAC, which exhibits peaks at 47 ppm (attributed to carbon signals near the carboxyl group) and 176 ppm (attributed to the carboxyl group). Fig. S1(b)† shows the ¹³C NMR spectra of LOCC, the peaks at 74, 66, 154, and 171 ppm are associated with the signals of carbons on the cyclic carbonate and the ester. Taken together, the FTIR and NMR characterization results demonstrate that the LOAC and LOCC were successfully synthesized.

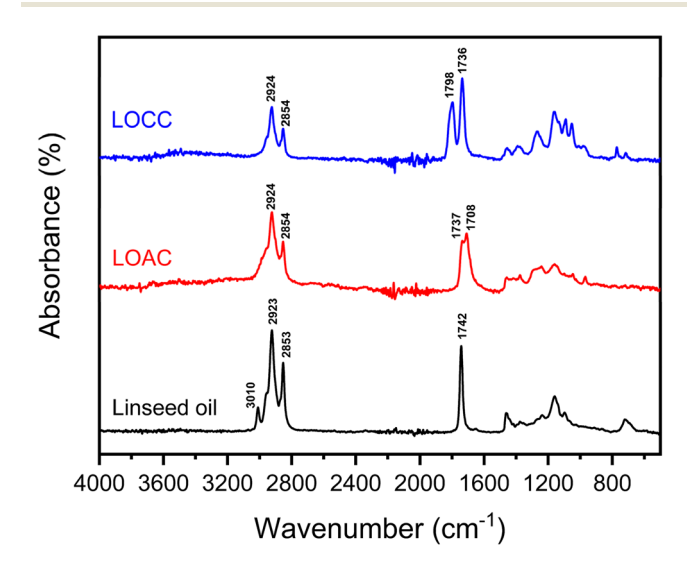
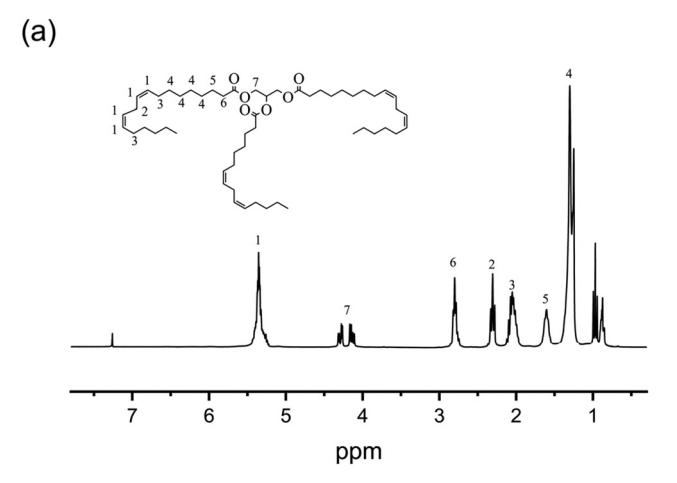
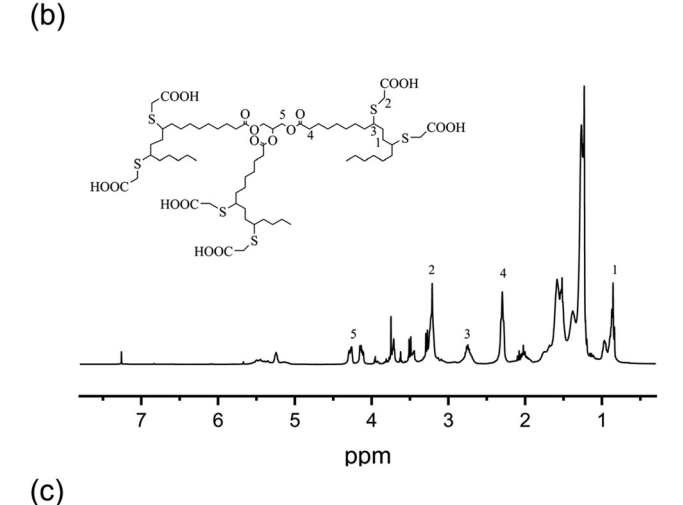


Fig. 1 FTIR spectra of linseed oil, LOAC, and LOCC.





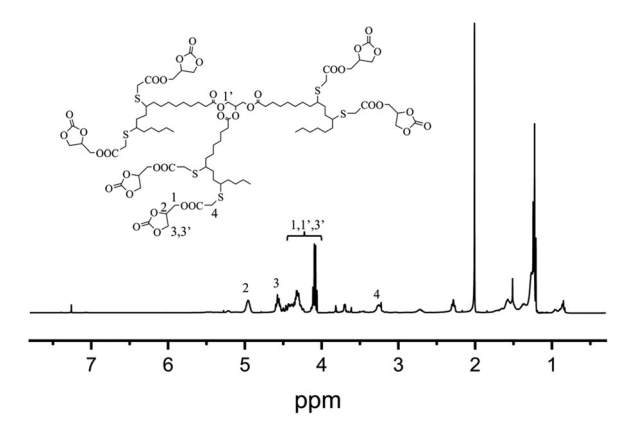


Fig. 2 ¹H NMR spectra of (a) linseed oil, (b) LOAC, and (c) LOCC.

Conversion of cyclic carbonates in linseed oil cyclic carbonate

Before being dispersed into the water, linseed oil cyclic carbonate (LOCC) was reacted with DMDPA and FDA at 75 °C for 6 h to obtain the NIPU prepolymer. The FTIR spectra of the mixture obtained before and after the cyclic carbonate–amine reaction are shown in Fig. S2.† The conversion of the cyclic carbonate groups was estimated based on the area of the C=O

stretching peak of cyclic carbonate at 1798 cm⁻¹. The peaks of C–H stretching at 2923 and 2853 cm⁻¹ were chosen as the internal reference. The conversion of cyclic carbonate was calculated using the following formula:

$$C = 1 - \frac{A_1/A_{\rm H}}{A_0/A_{\rm H}} \times 100 \tag{3}$$

where C is the conversion of cyclic carbonate; A_0 and A_1 are the peak areas of the cyclic carbonate functional group before and after the reaction, respectively; and $A_{\rm H}$ is the area of the peaks of C–H stretching. The values obtained for the conversion of the cyclic carbonate in NIPU-1, NIPU-2, NIPU-3, and NIPU-4 after the cyclic carbonate-amine reaction were 15.0%, 19.6%, 37.2%, and 44.1%, respectively.

Storage stability and particle size of NIPU dispersion

In this study, one solvent-borne NIPU and three waterborne NIPU dispersions were prepared. The average particle sizes for the three waterborne NIPU dispersions ranged from 115 to 136 nm, as shown in Fig. S3.† The storage stability of a waterborne NIPU dispersion was determined if sedimentation was observed during storage at room temperature. The results showed that NIPU-3 and NIPU-4 did not show any sedimentation after 3 months, whereas NIPU-2 showed sedimentation within 1 month. Moreover, no sedimentation was observed for NIPU-3 and NIPU-4 when centrifuged at 3000 rpm for 30 min, while sedimentation was evident for NIPU-2. For NIPU-3 and NIPU-4, more DMDPA was incorporated into the coating system; therefore, after neutralization, more ions were present at the particle surface, and these ions improved the hydrophily and stability of the coating.⁴¹

Characterization of NIPU films

After baking at 120 °C for 6 h, touch-free films were produced from the solvent-borne NIPU and the three different water-borne NIPU formulations. FTIR was adopted to characterize all four films, and the results are shown in Fig. 3. By comparing the FTIR spectra of the NIPU films in this figure with that for LOCC (Fig. 1), it can be noticed that new broad peaks were formed at 3600–3200 cm⁻¹ that are associated with the O-H stretching and N-H stretching, which resulted from the reaction between amine and cyclic carbonate (Fig. 3). The peak for LOCC at 1798 cm⁻¹ assigned to the C=O stretching of cyclic carbonate vanished, and a new peak at 1710 cm⁻¹ appeared in the spectra of the NIPU films, corresponding to the C=O stretching of the urethane group. 42,43 The disappearance and appearance of these typical signals confirmed the consumption of LOCC and the formation of NIPU.

Glass transition temperature

The glass transition temperature (T_g) of NIPU coating films was investigated by DSC. In the DSC curves presented in Fig. 4(a), only one T_g was identified for each NIPU sample, and the derivative DSC curve (shown in Fig. 4(b)) further confirmed this observation.⁴⁴ Moreover, within the testing temperature

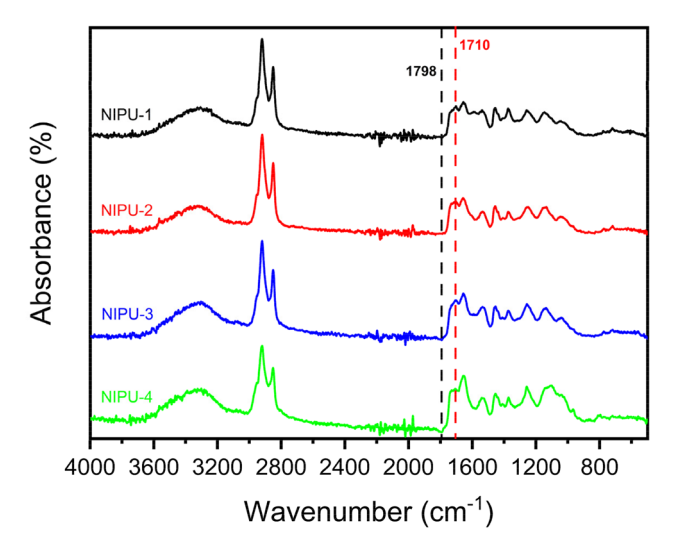


Fig. 3 FTIR spectra of the NIPU coating films (composition details are provided in Table 1).

range, no other characteristic signal was observed, which implies an amorphous structure for the NIPU films and indicates that all of the functional groups in the films were fully reacted.

The $T_{\rm g}$ values obtained for NIPU-1, NIPU-2, NIPU-3, and NIPU-4 were -9, 0, 6, and 11 °C, respectively. Based on these results, it is obvious that the $T_{\rm g}$ has increased with the increase in DMDPA content. This result is attributed to the reduced chain mobility for shorter chains as compared to that for longer chains. In addition, the higher DMDPA content results in a higher urethane group content, which leads to more hydrogen bonding. Therefore, a higher $T_{\rm g}$ was found for NIPU films with higher DMDPA contents.

Mechanical and thermal properties of NIPU films

DMTA analysis was utilized to investigate the viscoelastic properties of the NIPU films. Fig. 5 shows the storage modulus and loss factor as a function of temperature, where $T_{\rm g}$ is the temperature at which the loss factor was maximum within the temperature range. Table 2 lists the $T_{\rm g}$ and storage modulus within the glassy region (i.e., E' at -25 °C). The $T_{\rm g}$ obtained from DMTA shows the same trend as that obtained from the DSC results. The difference in the $T_{\rm g}$ results obtained from DSC and DMTA for the same NIPU film is attributed to the different testing methods.

The storage modulus describes the elasticity of materials. From Table 2, the E' value for the solvent-borne NIPU film (i.e., NIPU-1) was 1023 MPa, but the E' value for the waterborne film NIPU-2 was only 696 MPa. Solvent-borne coatings show better performance than waterborne coatings because of the differences in the film formation processes. For solvent-borne coatings, film formation occurs in a homogeneous phase that leads to a uniform film. However, film formation for waterborne coatings takes place in two inhomogeneous phases (a liquid phase and a solid phase), which may increase the

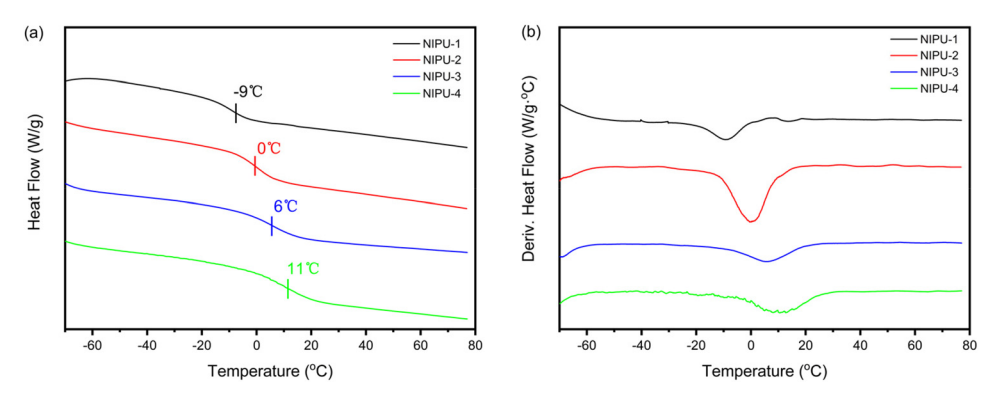


Fig. 4 (a) DSC curves and (b) derivative DSC curves for NIPU coating films (composition details are provided in Table 1).

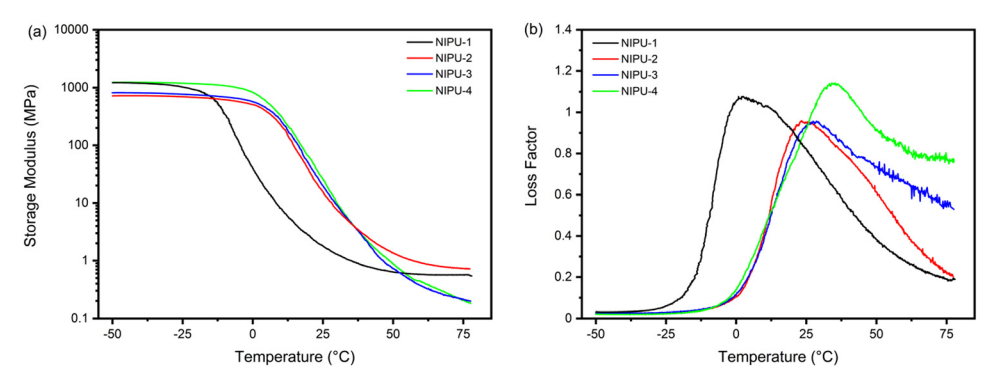


Fig. 5 (a) Storage modulus and (b) loss factor for the NIPU coating films.

Table 2 Glass transition temperature (T_g) and storage modulus (E') of the NIPU coatings from DMTA

	$T_{ m g}$ (°C)	E' (MPa)
NIPU-1	2	1023
NIPU-2	23	696
NIPU-3	28	769
NIPU-4	34	1194

chance to generate defects in the films. 45,46 For waterborne coatings, increasing the LOCC content results in a gradual increase in E' from 696 (in NIPU-2) to 1194 MPa (NIPU-4).

The elongation-at-break (ε) , tensile strength (σ) , and Young's modulus E for the NIPU coating films are listed in Table 3. The elongation-at-break decreased with the increase in LOCC and DMDPA content (from NIPU-1 to NIPU-4). The tensile strength and Young's modulus for NIPU-1 were slightly

Table 3 Thermal and mechanical properties of the NIPU coating films

	TGA (°C)		Tensile test results		
	T_{10}	T_{20}	ε (%)	σ (MPa)	E (MPa)
NIPU-1 NIPU-2 NIPU-3 NIPU-4	273 295 273 253	346 347 320 297	144.1 ± 12.2 119.5 ± 14 89.6 ± 15.5 68.3 ± 16.1	$\begin{array}{c} 0.39 \pm 0.04 \\ 0.32 \pm 0.04 \\ 0.41 \pm 0.14 \\ 0.55 \pm 0.14 \end{array}$	0.27 ± 0.03 0.26 ± 0.03 0.46 ± 0.09 0.82 ± 0.16

higher than those for NIPU-2; this may result from the formation of a film with fewer defects for the solvent-borne coating during the curing process. For the waterborne coatings, the σ and E changed from 0.32 and 0.26 MPa, respectively (for NIPU-2) to 0.55 and 0.82 MPa, respectively (for NIPU-4). The reason for the improved toughness of the polymer films is attributed to the higher content of urethane groups, which leads to more hydrogen bonding, thus increasing the physical

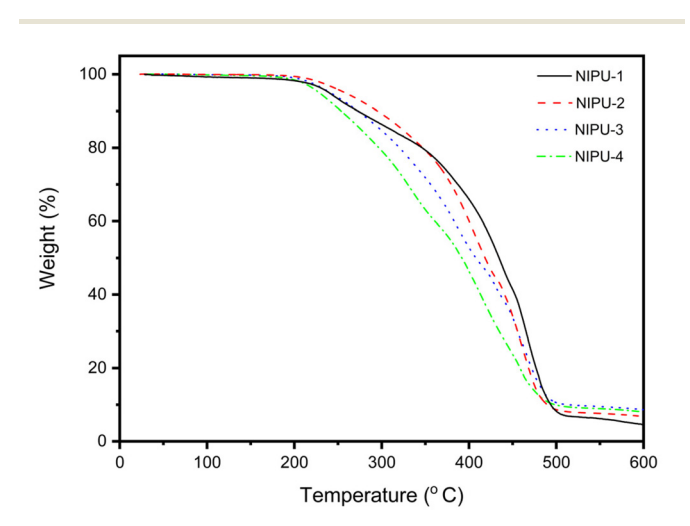


Fig. 6 TGA curves for the NIPU coating films.

Table 4 General coating properties of the NIPU coating films

	Dry film thick- ness (μm)	Pendulum hardness (s)	Pencil hardness	Solvent resistance	Reverse impact resistance (kg cm)	Crosshatch adhesion ^a	Pull-off adhesion (MPa)
NIPU-1	47.9	11	4B	100+	200+	4B	1.3 ± 0.2
NIPU-2	49.5	12	4B	100+	200+	4B	1.4 ± 0.1
NIPU-3	50.0	15	4B	100+	200+	4B	1.4 ± 0.1
NIPU-4	51.5	13	4B	100+	200+	4B	1.5 ± 0.2
Commercial WPII	57.3	53	НВ	100+	100+	ОВ	$\textbf{0.4} \pm \textbf{0.1}$

^a Crosshatch adhesion values range from 0B (worst) to 5B (best).

cross-linking. In addition, the higher content of DMDPA also improves the polarity of the polyurethane, leading to higher mechanical strength. Therefore, higher values for the storage modulus, σ , and E as well as lower values for elongation-atbreak were observed for NIPU-4 than for NIPU-3 and NIPU-2.

The thermal stability of the NIPU films was characterized by TGA, and the results are shown in Fig. 6. All NIPU films began decomposing at 220 °C and were fully decomposed at approximately 500 °C. The temperatures at 10% and 20% weight loss are also listed in Table 3. For NIPU-1, T_{10} and T_{20} were 274 °C and 346 °C, respectively; however, for NIPU-2, the values were slightly higher. T_{10} and T_{20} then decreased to 253 °C and 297 °C, respectively, for NIPU-4. The reduction of T_{10} and T_{20} from NIPU-2 to NIPU-4 could be explained by the different contents of urethane groups in the waterborne NIPU films. NIPU-4 was incorporated into more cyclic carbonate, which resulted in the formation of more urethane groups upon curing. Since urethane groups tend to decompose first under elevated temperatures, a NIPU with a higher content of urethane groups would be more easily decomposed.³⁹ In general, NIPU-1 (the solvent-borne NIPU) has a thermal stability that is higher than NIPU-3 and NIPU-4 but is comparable to that for NIPU-2. NIPU-2 has a similar thermal stability and an even higher T_{10} than NIPU-1, which may be due to the combined contributions from hydrogen bonding and urethane group content.⁴⁸

General coating properties

General coating properties of the synthetic NIPUs and commercial waterborne polyurethane (WPU) coating films-including pendulum hardness, pencil hardness, solvent resistance, impact resistance, crosshatch adhesion, and pull-off adhesion—are listed in Table 4. The viscosity of the coatings is presented in Fig. S4.† A commercial WPU with 27.4% solid content (Varathane 200241H Water-Based Ultimate Polyurethane) was purchased from Amazon. The commercial WPU was drawn down on the steel substrate with a wet film thickness of 120 µm, and it was cured overnight at room temperature. All coatings showed very high solvent resistance and impact resistance. In terms of hardness (pendulum hardness and pencil hardness), all NIPU samples showed hardness values that were similar but were much lower than that of the commercial WPU. The NIPU coating samples showed very strong adhesion to the steel panels (both crosshatch adhesion and pull-off adhesion), while the commercial WPU exhibited

much lower adhesion. The waterborne NIPU coatings (NIPU-2, NIPU-3, and NIPU-4) showed comparable performance to the commercial WPU; although they are softer than the commercial formulation, they presented better adhesion. The waterborne NIPU coatings also showed better reverse impact resistance than the commercial WPU, with a 200+ kg cm impact resistance. Overall, the waterborne NIPU coatings performed as well as the solvent-borne NIPU coating (NIPU-1) in terms of hardness, solvent resistance, impact resistance, and adhesion.

Conclusion

In this study, linseed oil-based waterborne NIPU coatings having a substantial bio-based content were successfully designed and synthesized. The linseed oil was transformed to linseed oil cyclic carbonate through a thiol-ene reaction followed by esterification. The cyclic carbonate was then reacted with bio-based FDA and DMDPA to obtain waterborne NIPU coatings with high bio-based content. By controlling the content of DMDPA, variation in the urethane content was induced. The resulting NIPU coatings showed different storage stabilities, particle size distributions, thermal properties, and mechanical properties. For waterborne NIPU coatings, the samples having higher DMDPA content showed better storage stability and more uniform particle size distributions. In addition, after curing, the coating films with higher DMDPA content showed higher $T_{\rm g}$ and mechanical strength but lower elongation and thermal stability. Despite the lower DMDPA content, the solventborne NIPU coating demonstrated superior mechanical properties to those for the waterborne coating NIPU-2. This finding can be attributed to the distinctions in the dispersant environment. Nevertheless, by adjusting the formulation, it was possible to produce waterborne NIPU coatings with properties that are comparable to those of the solvent-borne NIPU coating in terms of adhesion, solvent resistance, impact resistance, and hardness. The successful synthesis of highly bio-based waterborne NIPU underscores the potential of utilizing vegetable oils in NIPU coatings and paves the way for a novel direction in the advancement of vegetable oil-based waterborne NIPU coatings.

Conflicts of interest

There are no conflicts to declare.

Acknowledgements

The authors acknowledge the support from the U.S. National Science Foundation (NSF CAREER Award, #1943860). The authors appreciate the technical support from Dr. Lingyan Li at the National Center for Education and Research on Corrosion and Materials Performance. The authors also appreciate Sheila Pearson for her invaluable assistance in editing and proofreading this manuscript.

References

- 1 L. Zhang, Y. Huang, H. Dong, R. Xu and S. Jiang, *Composites, Part B*, 2021, 223, 109149.
- 2 Y. Yue, X. Gong, W. Jiao, Y. Li, X. Yin, Y. Si, J. Yu and B. Ding, *J. Colloid Interface Sci.*, 2021, **592**, 310–318.
- 3 C. Shen, Y. Cao, J. Rao, Y. Zou, H. Zhang, D. Wu and K. Chen, *Food Packag. Shelf Life*, 2021, 29, 100721.
- 4 H. Haridevan, D. A. C. Evans, A. J. Ragauskas, D. J. Martin and P. K. Annamalai, *Green Chem.*, 2021, 23, 8725–8753.
- 5 S. Li, S. Wang, X. Du, H. Wang, X. Cheng and Z. Du, *Prog. Org. Coat.*, 2022, **163**, 106613.
- 6 Polyurethane Market Size, Growth & Trends Report, 2022–2030, https://www.grandviewresearch.com/industry-analysis/polyurethane-pu-market, (accessed 28 July 2022).
- 7 P. Król, Prog. Mater. Sci., 2007, 52, 915-1015.
- 8 E. Dyer and H. Scott, J. Am. Chem. Soc., 1957, 79, 672-675.
- 9 X. Yang, S. Wang, X. Liu, Z. Huang, X. Huang, X. Xu, H. Liu, D. Wang and S. Shang, *Green Chem.*, 2021, 23, 6349-6355.
- 10 G. Coste, D. Berne, V. Ladmiral, C. Negrell and S. Caillol, *Eur. Polym. J.*, 2022, **176**, 111392.
- 11 B. Quienne, R. Poli, J. Pinaud and S. Caillol, *Green Chem.*, 2021, 23, 1678–1690.
- 12 I. Javni, D. P. Hong and Z. S. Petrović, *J. Appl. Polym. Sci.*, 2008, **108**, 3867–3875.
- 13 Y. Ecochard and S. Caillol, Eur. Polym. J., 2020, 137, 109915.
- 14 C. Carré, Y. Ecochard, S. Caillol and L. Avérous, *ChemSusChem*, 2019, **12**, 3410–3430.
- 15 C. Zhang, H. Wang and Q. Zhou, Green Chem., 2020, 22, 1329–1337.
- 16 International Agency for Research on Cancer, Re-evaluation of Some Organic Chemicals, Hydrazine, and Hydrogen Peroxide, IARC Monographs on the Evaluation of Carcinogenic Risk of Chemicals to Humans, IARC, Lyon, 1999, vol. 71, pp. 991–1013, http://monographs.iarc.fr/ENG/Monographs/vol71/mono71-43.pdf.
- 17 H. Khatoon, S. Iqbal, M. Irfan, A. Darda and N. K. Rawat, *Prog. Org. Coat.*, 2021, **154**, 106124.
- 18 M. A. R. Meier, J. O. Metzger and U. S. Schubert, *Chem. Soc. Rev.*, 2007, **36**, 1788–1802.
- 19 M. A. Mosiewicki and M. I. Aranguren, *Eur. Polym. J.*, 2013, **49**, 1243–1256.
- 20 I. Babahan-Bircan, J. Thomas and M. D. Soucek, *J. Coat. Technol. Res.*, 2022, **2022**, 1–16.

21 L. Hojabri, X. Kong and S. S. Narine, *Biomacromolecules*, 2009, **10**, 884–891.

- 22 X. Kong, G. Liu, H. Qi and J. M. Curtis, *Prog. Org. Coat.*, 2013, **76**, 1151–1160.
- 23 C. Zhang, H. Liang, D. Liang, Z. Lin, Q. Chen, P. Feng and Q. Wang, *Angew. Chem.*, *Int. Ed.*, 2021, **60**, 4289–4299.
- 24 A. Lee and Y. Deng, Eur. Polym. J., 2015, 63, 67-73.
- 25 X. Yang, C. Ren, X. Liu, P. Sun, X. Xu, H. Liu, M. Shen, S. Shang and Z. Song, *Mater. Chem. Front.*, 2021, 5, 6160– 6170.
- 26 W. Zhang, T. Wang, Z. Zheng, R. L. Quirino, F. Xie, Y. Li and C. Zhang, Chem. Eng. J., 2023, 452, 138965.
- 27 X. Liu, X. Yang, S. Wang, S. Wang, Z. Wang, S. Liu, X. Xu, H. Liu and Z. Song, ACS Sustainable Chem. Eng., 2021, 9, 4175–4184.
- 28 S. Doley and S. K. Dolui, Eur. Polym. J., 2018, 102, 161-168.
- 29 A. Cornille, R. Auvergne, O. Figovsky, B. Boutevin and S. Caillol, *Eur. Polym. J.*, 2017, **87**, 535–552.
- 30 C. E. Hoyle and C. N. Bowman, *Angew. Chem., Int. Ed.*, 2010, **49**, 1540–1573.
- 31 P. Jia, Y. Ma, H. Xia, M. Zheng, G. Feng, L. Hu, M. Zhang and Y. Zhou, ACS Sustainable Chem. Eng., 2018, 6, 13983– 13994.
- 32 C. Mokhtari, F. Malek, A. Manseri, S. Caillol and C. Negrell, *Eur. Polym. J.*, 2019, **113**, 18–28.
- 33 X. He, J. He, Y. Sun, X. Zhou, J. Zhang and F. Liu, *J. Coat. Technol. Res.*, 2022, **19**, 1055–1066.
- 34 N. Sukhawipat, N. Saetung, P. Pasetto, J. F. Pilard, S. Bistac and A. Saetung, *Prog. Org. Coat.*, 2020, **148**, 105854.
- 35 Y. Zhang, W. Zhang, H. Deng, W. Zhang, J. Kang and C. Zhang, ACS Sustainable Chem. Eng., 2020, 8, 17447–17457.
- 36 B. Quienne, R. Poli, J. Pinaud and S. Caillol, *Green Chem.*, 2021, 23, 1678–1690.
- 37 M. Desroches, S. Caillol, V. Lapinte, R. Auvergne and B. Boutevin, *Macromolecules*, 2011, 44, 2489–2500.
- 38 K. Li, Z. Liu, C. Wang, W. Fan, F. Liu, H. Li, Y. Zhu and H. Wang, *Prog. Org. Coat.*, 2020, **145**, 105668.
- 39 Z. Ling, C. Zhang and Q. Zhou, *Prog. Org. Coat.*, 2022, **169**, 106915.
- 40 S. Malburet, C. Di Mauro, C. Noè, A. Mija, M. Sangermano and A. Graillot, *RSC Adv.*, 2020, **10**, 41954–41966.
- 41 X. Wang, H. Liang, J. Jiang, Q. Wang, Y. Luo, P. Feng and C. Zhang, *Green Chem.*, 2020, 22, 5722–5729.
- 42 C. Zhang, H. Wang and Q. Zhou, Green Chem., 2020, 22, 1329–1337.
- 43 K. Huang, Z. Ling and Q. Zhou, J. Compos. Sci., 2021, 5, 194.
- 44 Q. M. Jia, M. Zheng, Y. C. Zhu, J. B. Li and C. Z. Xu, *Eur. Polym. J.*, 2007, 43, 35–42.
- 45 E. Brinkman and P. Vandevoorde, *Prog. Org. Coat.*, 1998, 34, 21–25.
- 46 A. Wegmann, Prog. Org. Coat., 1997, 32, 231-239.
- 47 P. Król, Prog. Mater. Sci., 2007, 52, 915-1015.
- 48 G. Vogt, S. Woell and P. Argos, *J. Mol. Biol.*, 1997, **269**, 631–643